Proceedings of the 7th International School

DEFECTS IN CRYSTALS

Szczyrk (Poland),
May 23-30, 1985

Edited by E. MIZERA

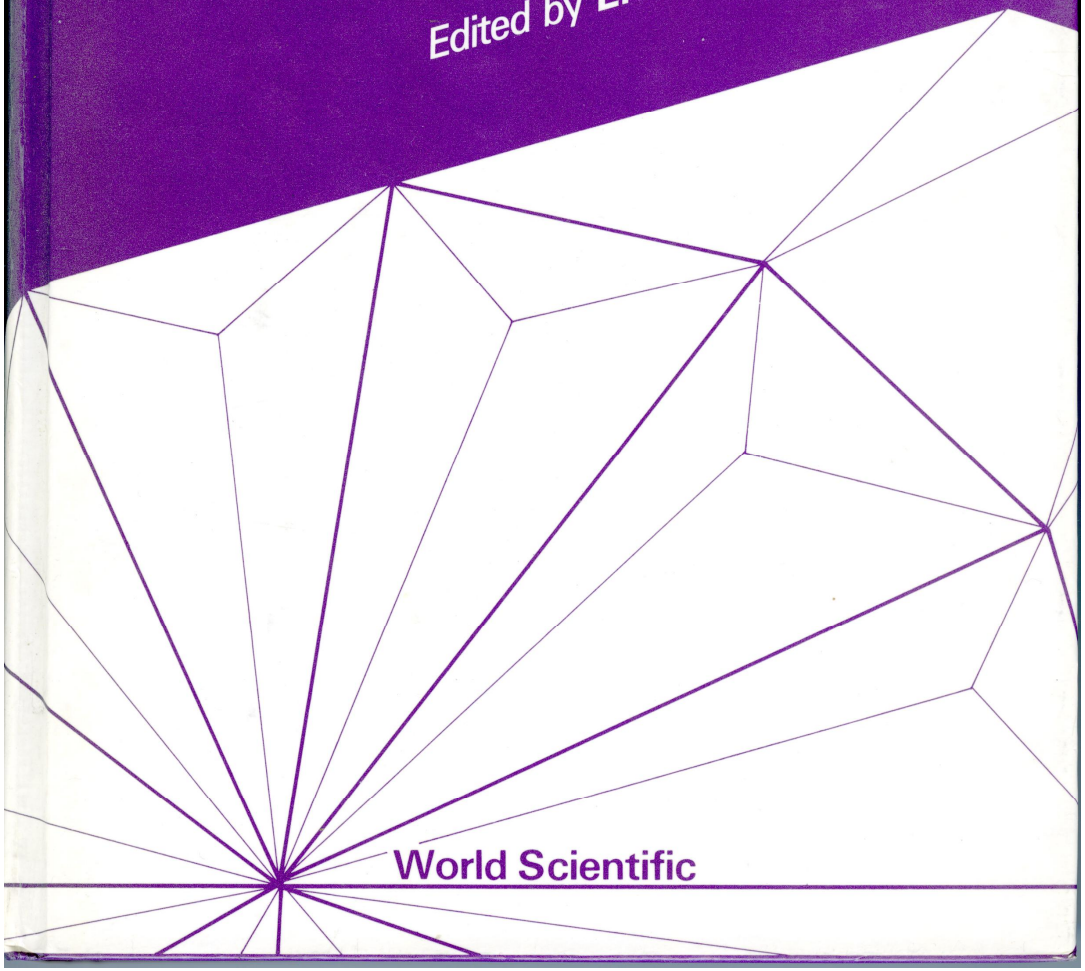

World Scientific

(Budapest, 1984)

|12| Shiojiri M. and Kaito C., JEOL news 21E, No.1, 2 (1983)

|13| Cowley J.M., Diffraction Physics, (North Holland, Amsterdam, 1975).

X-RAY AND HREM INVESTIGATIONS OF ZnS CRYSTALS

E. Mizera

Institute of Physics, Polish Academy of Sciences, Al.Lotnikow 32/46, 02-668 Warsaw, Poland

The results of X-ray diffraction analysis and high resolution lattice imaging of stacking faults in zinc sulphide crystals, grown by the Bridgman method and by chemical transport, are presented. Lattice images of the stacking faults, twins, ordered and disordered fragments of the structure of ZnS crystals are shown. This work deals only with an essentially geometric description of stacking faults and their distribution.

1. Introduction

Zinc sulphide is one of II-VI semiconductor compounds which crystallizes both in wurtzite (2H) and sphalerite (3C) structures. Perspective views of the absolute configurations (or polarities) in the wurtzite and sphalerite structures are shown in Fig. 1. [1].

The opposite polarity surfaces of wurtzite and sphalerite crystals are parallel to the (0001) and (111) planes, respectively. There is a close relation between the wurtzite and sphalerite structures. The atomic arrangements in both structures are very similar out to second-nearest neighbours.

The wurtzite structure (2H) can be described by means of the symbol sequence

```
aαbβaαbβaαbβaαbβ                h- interatomic layer in
A B A B A B A B                    wurtzite orientation
  h h h h h h                   A B A . . . B A B
                                  h . . . . . h .
```

The sphalerite structure (3C) is then characterized by the symbol sequence

$a\alpha b\beta c\gamma\, a\alpha b\beta c\gamma\, a\alpha b\beta c\gamma$ — c - interatomic layer in

A B C A B C A B C — sphalerite orientation

c c c c c c c c — A B C . B C A . C A B

. c . . . c . . . c .

where α, β or γ represent e.g. zinc, and a, b or c sulphur. Regarded as close-packed sequences, the wurtzite repeats after two double layers, the sphalerite after three.

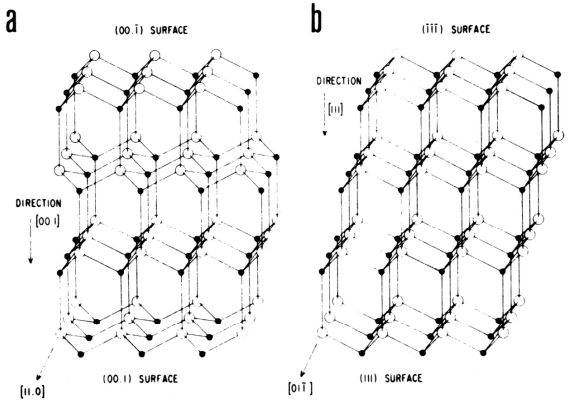

Fig. 1. Absolute configuration or polarity in the wurtzite (a) and sphalerite (b) structures.[1]
(small filled circles - S, large open circles - Zn)

It is usually assumed that the wurtzite is a high-temperature structure, while the sphalerite is a low-temperature one, the transition temperature between the two structures being 1020°C [2].

There is considerable scatter in the values reported for the lattice parameters of sphalerite and wurtzite polymorphic modifications of ZnS, the variations appear to be due both to impurities and to imperfections existing in real crystals.

It is well known that the stacking faults, twins and polytypes often occur in ZnS crystals.Though more than 140 polytypes have been identified in ZnS,the disordered (hc) structures were analysed only occasionally.

Stacking faults are frequent in II-VI crystals and are the principal defects in these compounds.

The nature of the stacking faults in real ZnS crystals is of interest because they are essential in the wurtzite-sphalerite phase transformation.

Two simple types of stacking faults are discussed in the literature (e.g. [1,3,8,9,10,11]). These are the growth (or random) faults and the deformation (or transformation) faults.

A growth fault in a wurtzite crystal forms a cubic lamella, one double layer thick

A B A B C B C ← "type I fault" [4]

h h c h h

Similarly, a growth fault in a cubic crystal forms a hexagonal layer

A B C A C B A ← corresponds to a twin

c c h c c

A deformation fault in a hexagonal sequence produces two adjacent cubic layers

A B A B C A C A ← "type II fault" [4]

h h c c h h

Similarly, two hexagonal layers are formed by shearing a cubic crystal

C A B C B C A B ← corresponds to an intrinsic stacking fault

c c h h c c

In a cubic crystal, we also distingush an extrinsic stacking fault, described by the sequence

A B C A C B C A B C

c c h c h c c c

The lattice images of stacking faults in ZnS crystals will be shown in Section 3.

Usually, ZnS crystals contain a large number of stacking faults. The occurrence of a large number of stacking faults in close-packed planes of wurtzite or sphalerite produces superstructures (fragments of one-dimentional ordered and disordered structures) which are known as polytypes. The detailed stacking sequence of some ZnS polytypes are given in Fig. 2. [1].

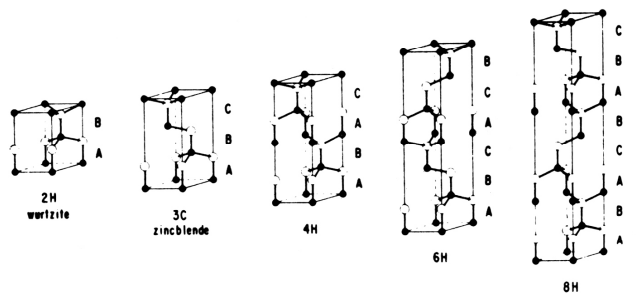

Fig. 2. Polytypes of ZnS. The letters A,B,C, locate the positions of the Zn-S layers.[1] (small filled circles - S, large open circles -Zn)

Polytypic structures may be classified into two groups:

i) polytypes - structures with well-defined unit cells (Fig. 2)

ii) disordered structures (DS), for which the stacking of layers is not periodically repeated.

All the polytypic structures have the same a - and b - dimensions of unit cells, but they differ from each other in the C - direction. The period in the C direction, which is perpendicular to the close-packed layer planes, is determined by the number of layers forming the repeated arrangement of layers.

$$C = n\,C_o$$

where n is the number of layers within a period, C_o is the minimum interplane distance (C_o in ZnS $\approx$ 0.313 nm for $0002_{(2H)}$, and $111_{(3C)}$ interplanar distances).

Polytypic modifications should be composed of identical structural unit layers and differ only in the stacking of layers. Each layer should have the same chemical composition, corresponding to the stoichiometry of the crystal. Each pair of adjacent layers is equidistant.

The structures of polytypes are usually described by the lattice constants, but may also be described by the parameters used for the disordered structures. i.e. the type of basic and

faulted arrangements of layers, density of faults, their distribution in the crystal, etc..

Defining e.g. the cubicity of the crystal as $\beta = (n_{c/N})\,100$ where n_c and N are the number of layers in the cubic orientation and the total number of layers in the disordered fragment of the crystal or in a unit cell of a polytype, respectively), it is found that the cubicities of all the ZnS polytype fragments and the disordered fragments lie between 50 and 100. This implies that all the disordered and polytype fragments of ZnS resemble a cubic structure. It seems that polytype and disordered fragments in ZnS are the ordered and disordered states of an incomplete wurtzite-sphalerite phase transformation.

In fact, ZnS single crystals 1 mm is size usually show several ordered and disordered fragments.

Polytypism was first found by Baumhauer in 1912 [2] , and until 1940 was presented as a phenomenon occuring only in SiC. Progress in the study of polytypism in inorganic crystals began in 1951, when Frank presented the screw-dislocation theory of crystal growth [5]. The first review of polymorphism and polytypism in crystals was presented in 1966 by Verma and Krishna [6].

Various explanations of the phenomenon of polytypism have been suggested from time to time. The theories of polytypism have been discussed in a number of original and review papers (e.g. [1,2,5,6,7,8,9,1o,11]). In recent years, several reports have appeared dealing with the theories of polytypism, based on statistical considerations [12,13].

Most of the existing theories of polytypism are simply theories of polytype formation. The disordered structures are regarded as destroyed (faulted) polytypes. The theories of polytypism which have received the most attention are the screw-dislocation theory of Frank [5] and the disorder -theory of Jagodzinski [7].

Up till now, most of the investigations performed in the field of polytypism have qualitative importance, while quantitative calculations are performed only occasionally .

Up till now, no unique theory of polytypism exists. In ZnS, the main process discussed was the formation of polytypes in the process of crystal growth from the vapour phase. The usually investigated ZnS crystals were synthesized from the vapour phase at the temperature of about 1200°C or less. The main methods used in the investigations of polytypes in ZnS were optical microscopy and X-ray diffraction analysis.

In this paper, the results of X-ray diffraction analysis and high resolution lattice imaging of stacking faults in zinc sulphide crystals, grown by the chemical transport and Bridgman methods are presented. Lattice images of stacking faults, twins, ordered and disordered fragments of the structure of ZnS crystals are shown.

This work deals only with an essentially geometric description of stacking faults and their distribution. A discussion of the physical processes of wurtzite-sphalerite phase transformation seems to be still too speculative, though little doubt, can exist about the fundamental role of the parameters (such as the temperature of crystal growth, stoichiometry of the crystals, impurities' concentration, vapour and/or mechanical pressure, role of dislocations) influencing this transition. It should be noticed in connection with this that the wurtzite-sphalerite phase transformation was directly observed [14] to be due to the expansion of partial dislocations. An example of how the partial changes the stacking sequence is shown further in this paper (Fig.16).

2. Experimental

The investigated zinc sulphide crystals were grown

i) by the Bridgman method from the stoichiometric melt under argon pressure (100 atm) at the temperature of 1820°C [15] and

ii) by the chemical (iodine) transport at various temperatures (between 700°C and 1160°C) [16].

X-ray diffraction analysis and high resolution electron microscopy (HREM) were used for studying the real structures of ZnS crystals grown by both methods.

The results of X-ray diffraction analysis and HREM investigations are presented below.

3. Results

3.1. X-ray diffraction analysis [15], [16]

The crystals were analysed by the X-ray oscillation method, using a cylindrical camera of 86 mm inner diameter. The crystals were oscillated around the c-axis in the range of 15°. Cu $K\alpha$ radiation was used. The intensity distribution of the 10.L spots was measured by a microphotometer.

To identify the stacking faults' distribution in the investigated crystals, the curves obtained by photometry of X-ray photographs were compared with those calculated theoretically which contained the appropriate proportions of stacking faults. The intensity curves which form the foundation of structural analysis were obtained from a structural model built up of 200 ± 5 layers. These models assume simple polytype cells and DS fragments. In each model, the structure is described by three independent parameters:

i) the percentage of layers arranged in simple polytype cells (20% 2H, 30% 3C, 40% 4H, etc.)

ii) %DS, i.e. the percentage of hexagonal layers appearing in fragments of the DS structures,

iii) the size of monopolytype fragments.

From the above, it is possible to find two additional parammeters

iv) the percentage of DS structure,

v) % α (hexagonality, % $\alpha = [h/(h+c)]$ 100, i.e. the percentage of hexagonal layers).

There are many possible interpretations of the stacking sequence in a crystal, which can be obtained from the calculated structural model. The structural model includes only some of the possible stacking layer sequences. The interference pattern obtained from complex structures is not the result of a simple addition of the interference pattern of the elements of the structural model. For these reasons, a given

experimental curve dose not always correspond to a single theoretical curve. A set of theoretical curves enables one to give limits within which the real stacking sequence of the crystal may be placed.

3.1.1. Real structure of ZnS crystals

All the ZnS crystals grown by the Bridgman method (i) (i.e. at the temperature of 1820°C) have revealed the sphalerite(3C) structure. The stacking faults and twins always occurred in crystals grown by this method. Hexagonality (%α) of the crystals was up to 7%. The stacking faults and twins extending across the crystals, were found to be distributed inhomogenenously. They form small groups, separated by large regions of untwinned material. In the investigated crystals, the density of dislocations was very low. Both dissociated and undissociated dislocations were observed, but only in the regions of untwinned material. No dislocation loops were observed in the investigated crystals. The dislocations in the as-grown crystals had the total Burgers vector of the (a/2) $\langle 110 \rangle$ type.

The structures found in ZnS crystals grown by chemical (iodine) transport (ii) are presented in Table 2 [16].

Structure of grown crystals: frequency of the appearance (in %) of a given structure in crystals for various growth temperatures

Temperature of growth (°C)	Structure												Number of samples	Th
	3C (%)	DS (5–10) (%)	DS (10–20) (%)	10H (%)	8H (%)	DS (20–30) (%)	6H (%)	DS (30–40) (%)	DS (40–50) (%)	4H (%)	2H (%)	Long period polytypes (%)		
(a) ZnS														
<800	100												3	0
800–850	88.7	5.8	3.9		1					0.6			18	1.6
860–880	75	13.9	4.4	0.6			0.6					5.5	18	3.1
890–910	54.7	10.3	8.8	1.7	1.6	2.5	6.4	6.2				7.8	32	10.5
920–940	70	7.3	11.7	0.4	9.4	1	0.2						24	5.1
950–970	19.7	12.4	26.9	4.4	4.6	15	13.1	2.6		1.3			27	16.6
980–1000			80	10				10					2	22.6
1010–1030		12.3	20.3	10.4	43.5	11.8	1.2						13	21.3
1040–1060				27.5		40	13.8	6.2	1.3	6.2	5		8	31
1070–1100													–	
1110–1160			46.1	8.3		38.4	7.2						9	20.6

Table 2. The structures of ZnS crystals grown by chemical transport; the frequency of appearance (in %) of a given structure in a crystal for various growth temperatures [16].

The dependence of the hexagonality (% α) on the growth temperature (T), for ZnS crystals grown by chemical transport, is shown graphically in Fig. 3.

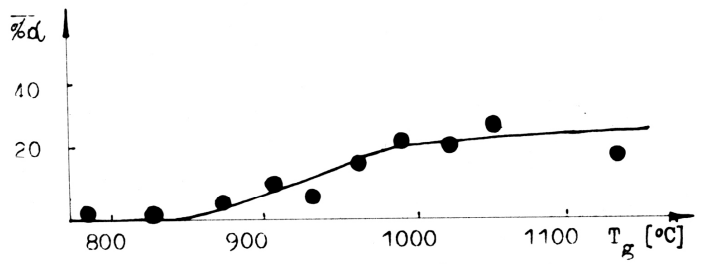

Fig. 3. Dependence of the parameter % α on the growth temperature (T_g) for ZnS crystals grown by chemical transport [16].

It is seen from the results presented in Table 2, that there is no apparent change in the parameter % α at around 1020°C (Fig. 3), although most authors regard this as the temperature of the wurtzite-sphalerite phase transformation. The parameter % α decreases steadily with decreasing growth temperature.

Most of the structures found in the crystals were of the nonperiodic (hc) type. Microscopic regions, containing periodic and nonperiodic structures, were found in the same crystal.

Pure sphalerite structure is the most favourable modification of ZnS crystals grown at lower temperatures (below 800°C -850°C). This confirms the earlier reports of other authors (e.g. [17]) that the range of stability of the sphalerite (3C) structure lies below 800°C.

In the temperature range between 800°C and 1160°C, a mixed (hc) structure (DS and polytype fragments) appears.

The structure of the crystals could be influence by the iodine atoms incorporated into them. The iodine content in the crystals may be very high; even of the order of 10^{-3}g/g [18]. However, this fact seems to be of minor importance, because

i) the structures of the crystals grown by iodine transport and by sublimation (at the temperature above 1100°C) are very similar,

ii) no relation between the iodine concentration in the growth system and the structure of the crystals has been found.

Thus, the resulting structure of ZnS crystals grown by chemical transport depends to a high degree on the temperature of crystallization. However, the effect of temperature cannot by unambiguously described.

For ZnS crystals grown by the Bridgman method (i.e. at the temperature of 1820°C), the sphalerite structure is the most favourable modification.

For the different methods (sublimation, chemical transport Taman or high pressure Bridgman methods) used for crystallization of ZnS crystals, the effect of temperature may be different.

Formation of the structures (% α layers) of ZnS crystals grown by different methods, in relation to the growth temperature (T_g), is shown schematically in Fig. 4.

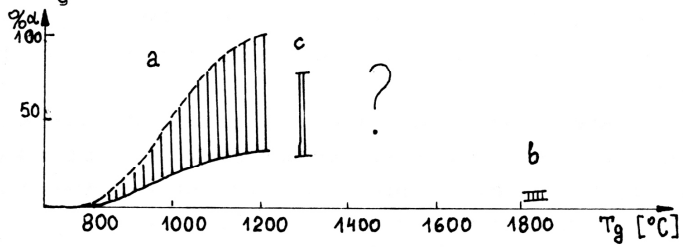

Fig. 4. Dependence of the parameter %α on the growth temperature (T_g) for the ZnS crystals grown by different methods [20], temperature ranges:
a) sublimation and chemical transport
b) Taman and high pressure Bridgman methods
c) [19].

In the temperature ranges a and b (Fig. 4), a number of factors - termodynamic, chemical, mechanical, geometrical, etc. - may influence the formation and stability of the structures of ZnS crystals.

Thus, for a discussion of the physical processes of wurtzite-sphalerite phase transformation, more extensive studies of the factors influencing the growth process of ZnS crystals are required.

3.2. HREM investigation

In this Section, the results of high resolution electron microscopy (HREM [21]) investigations of the crystals described in Section 3.1. are presented. Lattice images of stacking faults, twins, ordered and disordered fragments of the structure of ZnS crystals are shown.

The ⟨110⟩ oriented foils of sphalerite-type crystals were prepared by chemical polishing in CrO_3 + HCl solution, and by 3 keV Ar^+ ion bombardment. The ⟨110⟩ sphalerite-type, ⟨0001⟩ and $(11\bar{2}0)$ wurtzite-type oriented crushed thin crystal fragments were also examined.

The observations reported here were made with the Stockholm University JEM 200CX high resolution electron microscope, with the spherical aberration coefficient of 1.2 mm and Scherzer resolution limits of 0.25 nm. LaB_6 electron source was used. The images were recorded under axial illumination, using five, seven and more beams. The exposure time was 1 or 2 s.
The images were recorded at the magnification of 800 000. Micrographs of the stacking faults observed in sphalerite-type ZnS crystals are interpreted on the basis of the images of the known stacking faults in silicon [22,23,24,25].

3.2.1. Stacking faults in ZnS crystals and their distribution [26].

The sphalerite structure is best imaged with the [011] direction parallel to the electron beam. The projected potential distribution of the structure in this orientation is shown in Fig. 5a. Zinc and sulphur atoms in this projection are aligned in columns separated by 0.135 nm, according to the spacing of the (004) plane for ZnS, with the lattice parameter a = 0.540 nm determined by X-ray diffraction. Lattice image of the [011] -oriented sphalerite crystal (thin region less than 5 nm, the tunnels are light and the defocus is -63 nm / with the insert containing the computed image and the corresponding optical diffraction are shown

in Fig. 5b. and c., respectively. The Zn and S atoms are not separated in the image. Each image spot is asmetric / appears as a rectangular or elliptical blob /, reflecting the projected potential distribution.

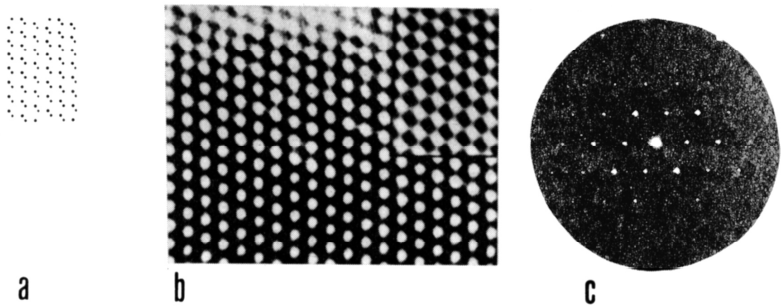

Fig. 5.a) [011] projected potential distribution of ZnS,
b) The [011] lattice image of ZnS with insert computed image,
c) The corresponding optical diffraction pattern.

The wurtzite structure is best imaged with the [0001] and $[11\bar{2}0]$ directions parallel to the electron beam. The lattice image of the wurtzite crystal in the $[11\bar{2}0]$ projection is shown in Fig. 6. The zinc and sulphur atoms (in this projection aligned in columns separated by 0.132 nm) are not separated in the image. Each image spot is asymmetric. The stacking sequence along the [0001] close- packed direction is indicated.

In Fig. 7, the lattice image of the wurtzite - type Al-doped ZnS crystal in the [0001] projection is shown.

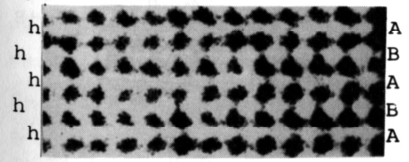

Fig.6. $[11\bar{2}0]$ lattice image of ZnS crystal. The tunnels are light. The stacking sequence is indicated.

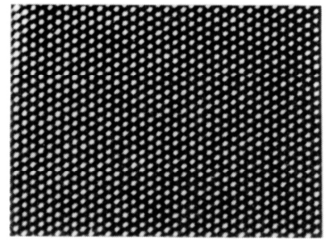

Fig.7. [0001] lattice image of Al-doped ZnS crystal.

The high resolution lattice images may show either dark or light contrast at the tunnel sites (or at the atomic columns), depending on focus and thickness. If thickness and defocus are both known for a particular image, the contrast can be calculated and compared directly with it. In interpreting images of defects, it is necessary to know whether the atomic columns (in this case, pairs of columns) are imaged with dark or light contrast. In interpreting lattice images of stacking faults in ZnS crystals, it is possible to exploit the geometrical arrangement of the atoms and tunnels at the known stacking faults in silicon. The variation of axial lattice images of intrinsic and extrinsic stacking faults in silicon with focus and thickness has been discussed in the literature [22,23,24,25]. Thus an careful inspection of the stacking faults discloses whether atom pairs (or tunnels) appear as dark or light contrast. This information is used directly for a description of the stacking faults in the investigated ZnS crystals.

The [0$\bar{1}$1] lattice images of intrinsic and extrinsic stacking faults in the sphalerite crystal are shown in Fig. 8a, and b, respectively. The stacking fault's contrast indicates that atom pairs are imaged with "black" contrast. The stacking sequences for the intrinsic (cchhcc) and the extrinsic fault (cchchcc) are indicated. An intrinsic fault consists of the absence of a plane in the stacking sequence. An extrinsic fault consists of an extra plane in the stacking sequence.

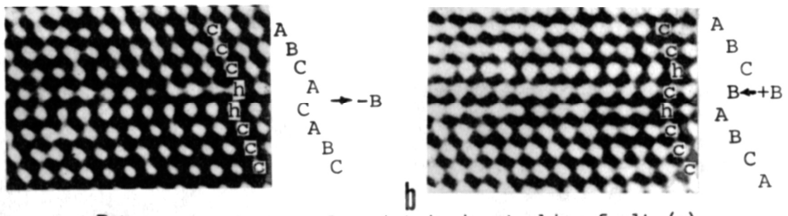

Fig. 8. (0$\bar{1}$1) lattice images of an intrinsic stacking fault (a) and an extrisnic stacking fault (b) in a ZnS crystal. The stacking sequences are indicated.

Lattice images of an extrinsic fault, with "black" and "white" atom pairs contrast, are shown in Fig. 9.a. and b.

respectively. An extrinsic fault terminating in a Frank partial dislocation at the left and in two Shockley partials at the right is shown in Fig. 10.

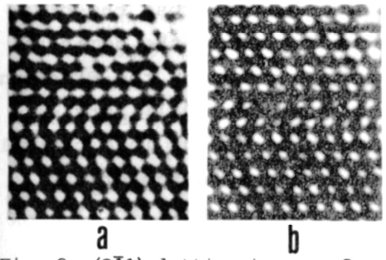

Fig. 9. (0$\bar{1}$1) lattice images of an extrinsic stacking fault, with "black" (a) and "light" (b) contrast, in a ZnS crystal.

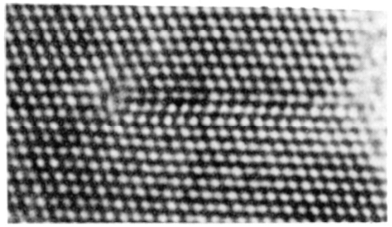

Fig. 10. (0$\bar{1}$1) lattice image of an extrinsic fault terminating in a Frank partial at the left and in two Shockley partials at the right.

An intrinsic stacking fault and a 30° partial of a dissociated screw dislocation, imaged with "black" and "white" atom pairs contrast, are shown in Fig.11.a. and b., respectively. A comparison of the experimental images of Fig.11. with e.g. the computed images of a 30° partial in silicon of Fig. 6.[23] or Fig. 7 [25] suggests that the 30° partial in ZnS is of glide type.

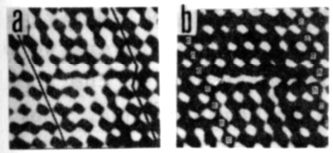

Fig. 11. (0$\bar{1}$1) lattice images of an intrinsic stacking fault terminating in a 30° partial. (a) "black " and (b) "light" contrast.

Twin boundaries in a ZnS crystal imaged with "white" and "black" atom pairs contrast, are shown in Fig. 12a. and b., respectively. Each of the boundaries is formed by a stacking fault ("growth" fault (cchcc)) introduced into crystal).

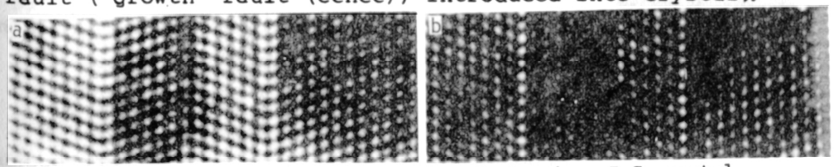

Fig.12. (011) lattice images of twin boundaries in a ZnS crystal, (a) "white" and (b) "black" contrast

Fig. 13. $(O\bar{1}1)$ lattice image of twins in a ZnS crystal grown by the Bridgman method.

Narrow twins, extending across the crystals in separated groups, were the dominant defects in ZnS crystals grown by the Bridgman method (i). Fig. 13 shows the $(O1\bar{1})$ lattice image of a group of narrow twins in a crystal grown by this method. The sequence of the (hc) layers for the region imaged in Fig. 13 is as follows: (from the top to the bottom part of the image)

10c h 14c h 10c h 3c h 3c h 3c h ch ch ch 3ch
3c h 2c h 5c h 6c h 11c h c h c h 3c h 10c

In this twinned region of the crystal:
i) %h layers ~ 14% (total number of layers = 129, number of hexagonal layers = 18),
ii) short and long period arrangements of cubic layers are observed,
iii) sequences: (cchcc) - corresponds to the twin, (hchchc) - corresponds to the extrinsic fault (cchchcc) or to the 4H polytype (hchchc) (hccchccc) - corresponds to the 8H polytype.

The distributions of the (hc) layers were different in each twinned region of the ZnS crystals grown by the Bridgman method. They were, for example, as follows:

i) 11c h 6c h 2c h 10c h 13c h 10c h 4c h 2c h 14c h 14c h 2c h c h c h 5c h 3c h 4c h 2c h 11c h 11c h 5c h 5c h c h 2c h c h 2c h 8c h 2c h 5c h 9c h 2c h 5c h 2c h 5c h 6c h 2c h c h 15c h 2c h 3c h c h 4c h 2c h
In this twinned region of the crystal:
%h layers = 17% ((h + c) layers = 258, h layers = 43), sequences: (cchcc) - corresponds to the twin, (cchchcc) - corresponds to the extrinsic stacking fault or 4H polytype. Adjacent identical sequences of the

(hc) layers occurred in this region: e.g. (14c h 14c h), (11c h 11c h), (5c h 5c h) and long period arrangement of (hcchccccc) layers - (hcchcccchcchccccc).

ii) 12c h 2c h 3c h 4c h 2c h 2c h 4c h 2c h 2c h 2c h 10c h 5c h 2c h c h 2c h c h 30c h 14c h 12c
In this region of the the crystal:
%h layers = 14% (h + c) layers = 130, h layers = 18), sequences: (cchcc) - corresponds to the twin, (cchchcc) - corresponds to the extrinsic stacking fault or 4H polytype. Adjacent identical sequences of the (hc) layers occurred in this region: (hcchcchcc) - sequence corresponds to the 6H (hcchcc) polytype, (hcchchcchch) - long period arrangement of (hcchc) layers, (hcccchcchcchcccchcchcch) - long period arrangement of the (hcccchcchcc) layers.

In the three twinned regions discussed here, no 2H or intrinsic stacking fault ((cchhcc) "deformation" fault) sequences of layers were observed.

A distribution of the (hc) layers similar to that in the twinned regions of the Bridgman-grown crystals was observed for the crystals grown by chemical transport, with comparable or smaller number of hexagonal layers. The distribution of the (hc) layers in the crystals grown by chemical transport was inhomogeneous. In microregions of these crystals, the number of hexagonal layers was much higher than the mean number determined by X-ray diffraction. In the investigated crystals the mean number of (h) layers determined by X-ray diffraction was up to 30% (Table 2).

A microregion of a ZnS crystal grown by chemical transport with a high number of hexagonal layers is shown in Fig. 14. The sequence of the (hc) layers for the region imaged in Fig. 14 is as follows (from the top to the bottom part of the image):

c hh cc hh c h c h c h c h c h c h c h c h c h c h c h c h
cc hh c hh c h cc h cc hh c h c h c h c h c h c h cc hh c h
c hhhhh cc hh c h c h cc hh c h c h cc hh c h c h c h c h c
h c h c h c h c h c h c h c h cc hh cc hh cccc

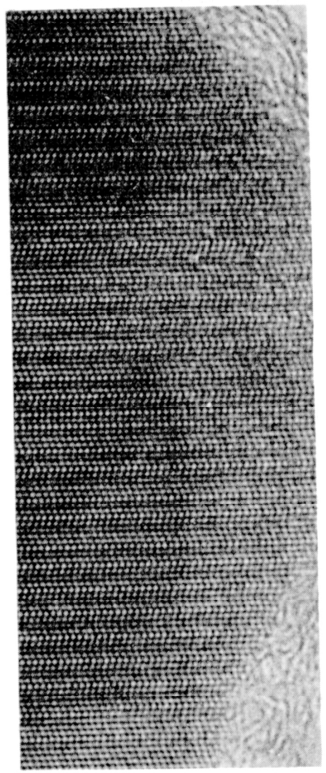

Fig. 14 Lattice image of a ZnS crystal grown by chemical transport. The stacking sequence is indicated (see text).

$(01\bar{1}) \| (11\bar{2}0)$

$[111]_{(3C)} \| [0001]_{(2H)}$,

In this region of the crystal:
%h layers ~ 50%, (h + c) layers = 127, h layers = 64),
sequences: (ccccc)-corresponds to the 3C structure, (hhhhh) corresponds to the 2H structure, (cchcc)-corresponds to the twin ("growth" fault),
(cchhcc)-corresponds to the intrinsic stacking fault ("deformation" fault), (chchch)-corresponds to the extrinsic stacking fault (cchchcc) or 4H (hchchc) polytype, (hcchcc)-corresponds to the 6H polytype, (cchhchch cchhchch cchhchch)-long period arrangement of the (cchhchch) layers.

In terms of the commonly used description of polytype structures, one can say that, in this region of the crystal,

fragments of the 3C, 2H, 4H, structures and the long period (cchhchch) arrangement of layers occur simultaneously.

In Fig. 15 which present enlarged fragments of Fig.14, imaged with "black" atom pairs contrast, are shown the 2H, 4H and long period (cchhchch) arrangements of layers. The stacking sequence of the (hc) layers is indicated.

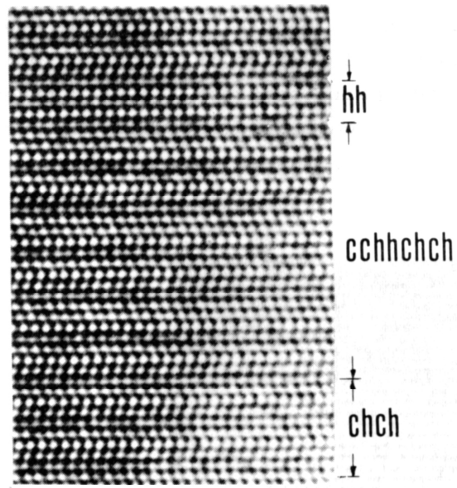

Fig. 15. Enlarged fragment of Fig.14. The stacking sequence is indicated.

From the above experimental example (Fig.14) of the distribution of the (hc) layers in a fragment of the crystal containing a comparable number of (h) and (c) layers, one can draw following conclusions:

- the 2H and 3C structures may occur simultaneously in the same crystal,
- the commonly used classification of stacking faults into the "growth" and "deformation" faults is useless when the number of (h) and (c) layers are comparable,
- both the (cchcc) - "growth" and the (cchhcc)- "deformation" sequence of layers occur in the crystals,
- a classification of stacking faults into twins (cchcc), intrinsic faults (cchhcc) and extrinsic faults (cchchcc), being typical defects in a sphalerite structure, is more

useful. The (cchcc), (cchhcc) and (chchc) stacking sequences are actually observed in the crystals.

- In a real crystal, when many factors have influence the crystal growth process, the number of the different possible distributions of the (hc) layers may be practically unlimited.
- In mixed (hc) structures partial dislocations have been observed. An example of how a partial changes the stacking sequences is shown in Fig. 16, which is fragments of Fig.14, imaged with "black" atom pairs contrast. In this fragment of crystal, the introduced partial drastically changed the arrangement of the (h) and(c) layers. The stacking sequences are indicated.

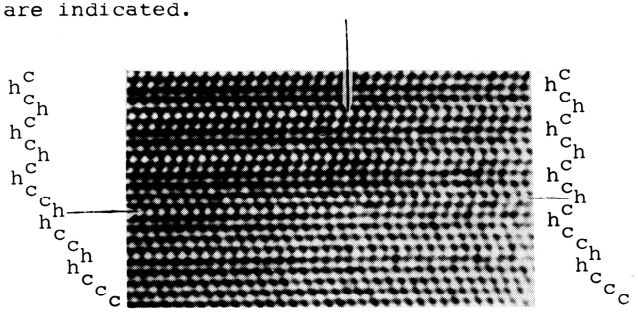

Fig. 16. Enlarged fragment of Fig. 14. The introduced partial chages the stacking sequences. The stacking sequences are indicated.

- It seems that the independent (individual) partial dislocations take part in the formation of the structure during the crystal growth. A steady creation and/or movement of the partials will introduce stacking faults at regular or irregular intervals in the structure thus leading to a phase transformation.

Acknowlegements

The author is grateful to Dr.M.Demianiuk, Dr.M.J.Kozielski and Dr.B.Pałosz providing the ZnS crystals. I thank Dr.M.Sundberg, P.Werner and B.Hillebrand for cooperation in HREM investigations of II-VI compounds. I would like to thank Prof.J.Auleytner, Prof.L.Kihlborg and Prof.J.Heydenreich for use the microscopes and other facilities at their Institutes.

REFERENCES

[1] Roth W.L., in Physics and Chemistry of II-VI Compounds, ed. Aven M. and Prener J.S., North-Holland Publ.Co., 1967
[2] Baumhauer H., Z.Krist., 50, 33 (1912)
[3] Hirth J.P. and Lothe J., Theory of Dislocations, Wiley and Sans New York 1982
[4] Blank H., Delavignette P., Gevers R., and Amelinck S., phys.stat.sol. 7, 747 (1964)
[5] Frank F.C., Phil.Mag., 42, 1014 (1951)
[6] Verma A.R. and Krishna P., Polymorphism and Polytypism in Crystals, Jhon Wiley, New York, 1966
[7] Jagodzinski H., Neues Jahrb.Miner.Monatsh, 3, 49 (1954), Acta Cryst. 2, 201, 298 (1949) and 8, 279 (1954)
[8] Trigunayat C.C. and Chadha G.K. phys.stat.sol.(a) 4, 9, (1971)
[9] Rai K.N., phys.stat.sol.(a) 8, 271 (1971)
[10] Pałosz B., phys.stat.sol.(a) 77, 11 (1983)
[11] Pandey D. and Krishna P., Current Topics in Materials Science Vol.9, Chapter 2, ed.E.Kaldis North-Holland Publ. Co., 1982
[12] Uppal M.K., Ramasesha S. and Rao C.N.R. Acta Cryst.A36, 356 (1980)
[13] Kozielski M.J. and Tomaszewicz A., Bull.Acad.Pol.Sci. Sér.Math.Astr.Phys. 26 749 (1975)
[14] D'Aragona F.S., Delavignette P. and Amelinckx S., phys.stat.sol.(a) 14, K115 (1966)
[15] Kozielski M.J., J.Cryst.Growth. 30, 86 (1975)
[16] Pałosz W., Kozielski M.J., and Pałosz B., J.Cryst. Growth 58, 185 (1982)
[17] Baars J. and Brandt G., J.Phys.Chem.Solids 34, 905 (1973)
[18] Hartmann H., J.Cryst.Growth 42, 144 (1977)

[19] Hartmann H., Kristal und Technik 1, 27 (1966)
[20] Kozielski M.J., private discussion
[21] Spence J.C.H., Experimental High-Resolution Electron Microscopy, Clarendon Press, Oxford 1981
[22] Rez P. and Krivanek O., Proceedings of Ninth International Congress on Electron Microscopy, Toronto Vol.1, p.288 (1978)
[23] Olsen A. and Spence J.C.H., Phil.Mag., A43, 945 (1981)
[24] Chiang S.W., Carter C.B. and Kohlstedt D.L., Phil.Mag. A42, 103 (1980)
[25] Hutchison J.L., Ultramicroscopy 9, 191 (1982)
[26] Mizera E. and Sunberg M., Proceedings of Eight European Congress on Electron Microscopy, Budapest Vol.2, p.945 (1984)

DEFECT STATES IN IV-VI SEMICONDUCTORS

K. Lischka

Institut für Experimentalphysik, Johannes Kepler Universität Linz, A-4040 Linz, Austria

Experimental investigations of defect states in IV-VI semiconductors, preferentially the lead salt compounds, are reviewed. The emphasis is laid on recent investigations, which have revealed a number of outstanding properties of intrinsic point defects and impurities.

1. Introduction

The semiconducting compounds of group IV and VI elements, the lead, tin and germanium salts, have attracted some interest both from the basic and the applied points of view. Concerning basic physics, the IV-VI compounds have quite outstanding properties when compared with standard semiconductors (group IV, III-V and II-VI compounds). The lead salts have 10 valence electrons per unit cell and crystallize in the rock salt structure with an octrahedral coordination of the next neighbour atoms [1]. The lead salts are direct gap semiconductors, with multivalley conduction and valence band extrema at the L-point of the Brillouin zone. Some ternary compounds exhibit a zero gap transition which is, however, not symmetry-induced as in II-VI compounds, but is due to an accidental degeneracy of the conduction and valence bands. Another outstanding property of the lead salts is their high dielectric constant, which reflects their tendency to undergo a ferroelectric phase transition [2]. The technological interest in the lead salt compounds is based on their use for the production of